Harla Journals

Harla Journal of Applied Science and Materials

Journal home page: https://journals.ddu.edu.et/index.php/HJASM

Harla journal of Applied Science and Materials

CFD Modelling and Thermal Performance Analysis of Ventilated Double Skin Roof Structure

Abdou Idris[1]*, Abdoulkader Ibrahim[1] and Assabo Mohamed[1]

[1]Université de Djibouti, Faculté d'Ingénieurs, Djibouti

Abstract

Air conditioning is a serious issue in hot areas. The demand to live in more comfortable buildings, which is understandable, has resulted in an increase in energy consumption by air conditioning. However, in Djibouti, one of the world's most expensive electricity countries, this demand is exacerbated by building that is inadequate and unfit for the climate. This paper investigates the design of the roof which is the surface receiving the most solar radiation and which determines the general behaviour of the building. The energy performance of a double skin ventilated roof is modeled and analysed using Computational Fluid Dynamics (CFD). This study looks at Djibouti's climate, which is hot and humid in the winter and extremely hot and humid in the summer. To characterize the flow and heat transfer induced in the ventilated roof in a steady state, roof simulations are carried out using the Ansys Fluent software. The effects of numerous parameters on heat gain through the roof are compared, including the internal emissivity of the upper surface, the thickness of the roof insulation, and the thickness of the vented channel. The energy saving potential is also studied and presented in comparison to the current constructions in Djibouti.

Keywords: Double skin roof; CFD; Energy saving; Forced convection; Natural convection.

1. Introduction

Construction elements such as double-skin roofing can be used for more than one purpose at the same time and can reduce the energy requirements of a building. Such structures have the potential to be used in a bioclimatic approach, especially in Djibouti and other high-solar-radiation areas. With 90 percent of overall electricity usage in Djibouti, the construction sector is by far the largest (ADME, 2013). Cooling demands, such as air conditioning and ventilation, continue to dominate electricity demand, contributing for more than 70% of total consumption.

The study of ventilated structures is quite complicated and is dependent on many variables such as airflow rate, thermo-physical properties of materials, external conditions, and so on.

* *Corresponding author: Abdou Idris; Email: abdou_idriss_omar@univ.edu.dj*
Doi: https://doi.org/10.20372/hjasm.v1i2.47

Received: March 2022; Received in revised form: April 2022; Accepted: May 2022

Since Fracastoro *et al.* (1997), who examined the idea of reducing heat gain in buildings by employing under-roof cavities, much research has been done to study the performance of a ventilated roof.

They performed a steady-state thermal analysis of ventilated and unventilated light roofs using a numerical model. The relationship between solar heat input and induced cavity ventilation rate was studied by Sandberg and Moshfegh (1998). Since Fracastoro *et al.* (1997), who examined the idea of reducing heat gain in buildings by employing under-roof cavities, much research has been done to study the performance of a ventilated roof. They performed a steady-state thermal analysis of ventilated and unventilated light roofs using a numerical model. The relationship between solar heat input and induced cavity ventilation rate was studied by Sandberg and Moshfegh (1998). Hirunlabh *et al.* (2001) investigated different Nusselt number correlations as a function of solar radiation for various roof tilt degrees. A set of measurements were taken on an experimental double-skin roof by the French Scientific and Technical Centre for Building Research (CSTB, 2002). Khedari *et al.* (2002) experimental investigation of free convection in a roof solar collector reveals a Nusselt number dependence law on the Rayleigh number, the angle of the channel, and the aspect ratio of the ventilation cavity, i.e., the ratio of the channel's width to its length. Ciampi *et al.* (2005), then, Dimoudi *et al.* (2006) and Černe and Medved (2007) observed 50 that the ventilated roof contributes to keeping the temperature of the inner surface closer to ambient conditions, reducing the impact of solar radiation on the building.

Chang *et al.* (2008) investigated the energy savings achieved by adding a radiant barrier system in a double-skin roof in an experimental setting. Biwole *et al.* (2008) suggested that the appropriate width for the ventilation channel must be between 6 cm and 10 cm based on numerical and experimental modeling. Using an open-ended inclined model with parallel plates to replicate the ventilated roof structure receiving solar radiation Lai *et al.* (2008) examined the ideal spacing as a function of the Grashof number. For their part, Villi *et al.* (2009) constructed correlations for describing airflow and heat transport phenomena in the ventilated cavity. Gagliano *et al.* (2012) concluded that roof ventilation can significantly lower heat fluxes (up to 50%) during the summer season based on a research of the thermo-fluid dynamic behavior of air within ventilated roofs and heat fluxes through ventilated roofs.

The thermal analysis of a ventilated roof requires both a complete thermo-aeraulic analysis of the air gap and accurate knowledge of the heat transfer coefficients as well as the thermo-physical properties of the materials. Most of the studies presented previously use simplified numerical models whose boundary conditions have not been completely mastered. The uncertainty of the internal and external heat transfer coefficients of the ventilated roof and of the head losses within the channel, for example, can reduce the reliability of the CFD analysis. This study completes our previous paper (Omar *et al.*, 2017) and differs from all previous studies because we considered the entire building to analyze the thermal behavior of the ventilated roof.

The objective of this paper is to study the thermal performance of the ventilated roofs solution in Djibouti. The airflow and heat transfer processes in the ventilated cavity with buoyancy driven airflow and forced convection were characterized using CFD.

2. Methods

2.1. Model Description

Building typology in Djibouti has traditionally focused on the growth of two sectors: residential and tertiary. The residential sector consists of the following categories of structures: In most cases, a standard home's roof is made composed of sheet metal or tiles. This kind accounts for 90% of the residential sector in Djibouti, according to DISED, the Djiboutian agency for demographic and statistical data (DISED, 2015) as shown in figure 1 (a). Figure 1 (b) shows an example of a building front face with a pitch angle of at least 5 degrees. Residential buildings made up 2% of the total construction and had many floors and a concrete roof

- Residential buildings made up 2% of the total construction and had many floors and a concrete roof.
- Villas, which are single-family dwellings with a tiled or concrete roof, account for 3% of all structures. The previous structures' walls are made out of external and internal cement plaster, as well as bricks or concrete blocks.
- Tukuls are unofficial settlements that make up more than 5% of all building. They are highly fragile structures located in an urban slum.

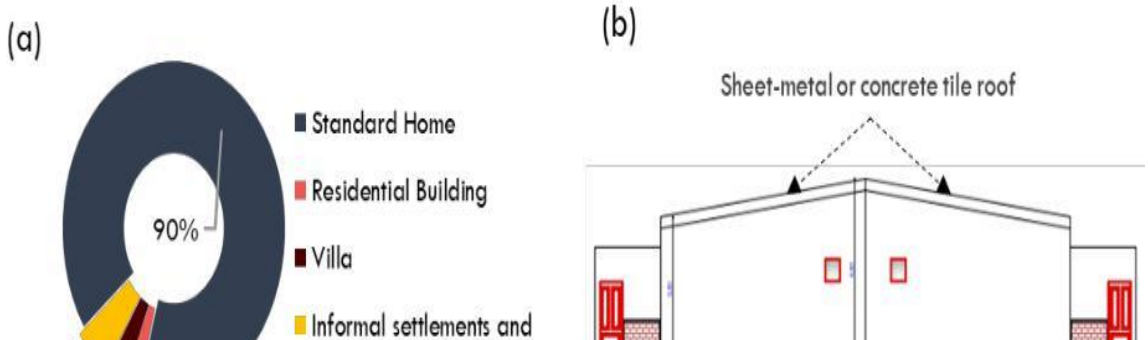

Figure 1. (a) Different types of construction in Djibouti; (b) Example of the building with the largest share

The current mode of construction in Djibouti offers quite of potential for improving thermal efficiency. Despite the lack of traditional architecture in Djibouti, which could have served as the foundation for a sober bioclimatic design in terms of resource use and energy consumption, the crossing of the city of Djibouti still makes it easy to discover bioclimatic architectural details: Natural ventilation forcing in buildings which use perforated bricks, shading by shutters, brise-soleil for windows shading, among others. In this study, we are interested in the roof of a standard house since it represents the largest part of the building typology in Djibouti. The roof of this style of structure is usually made of peaked galvanized sheet metal. Two model configurations to reduce the heat fluxes through the roof were considered. The first configuration, as illustrated in Figure 2, is a ventilated structure made up of two flat parts separated by an air gap that allows air to pass. The conventional roof is covered with a 6-mm screen (outside surface). Insulation is applied to the inner slab in the second configuration.

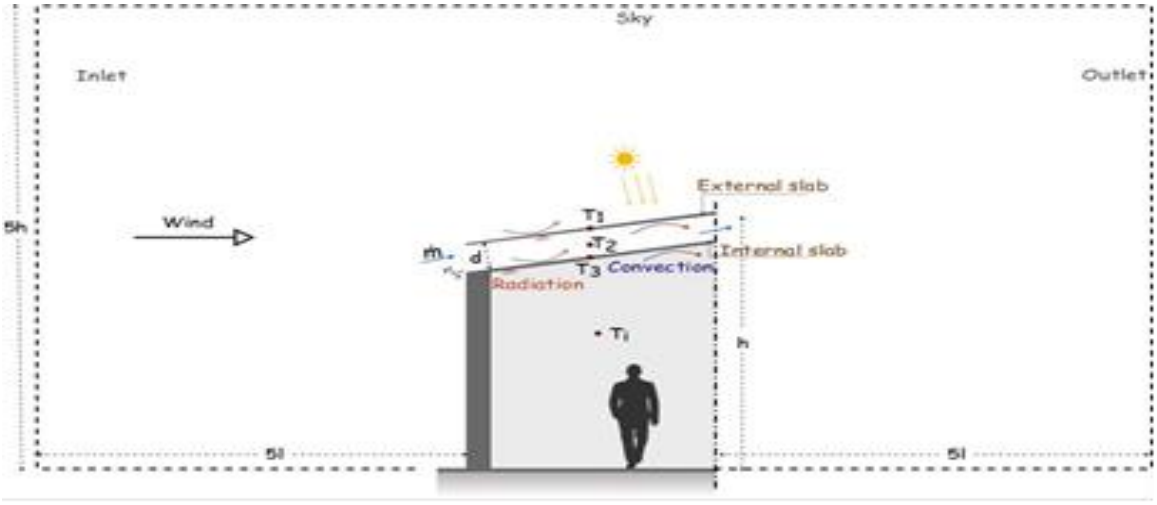

Figure 2. Ventilated double skin roof model.

The Thermo-physical characteristics and geometry of the ventilated roofs are shown in Table 1. All materials have been assumed to be homogeneous and isotropic.

Table 1. The Thermo-physical characteristics and geometry of the ventilated roofs

Cases	Cp, J/(kg.K)	λ, W/m.K	ρ, kg/m^3	d, m
Outer slab	500	61	7520	0.006
Inner Slab	500	61	7520	0.006
Airgap	1006	0.025	1.23	0.1; 0.2
Insulation	1400	0.035	25	0.02; 0.05; 0.1

Where Cp is Specific heat [J/ (kg. K), d is thickness of air gap (m), λ is thermal conductivity [W/ (m.K)] and ρ is density (kg/m^3).

A non-ventilated air gap separates the roof from the inside. The air gap's thermal resistance was calculated to be 0.18 m²/ (K.W), according to ISO EN UNI 6946 norms (CEN, 2007). CFD prediction also confirmed this figure.

2.2. CFD Modelling

Local wind data, building density, and geometry all influence wind conditions in the urban environment (Antvorskov, 2008; Abdou Idris *et al.*, 2016). These can make the contribution of wind difficult to estimate. However, despite the difficulty, it may be possible to study a case of calculation in forced convection in the present analysis. Then, in order to achieve more general conclusions, only the flow of air due to density differences caused by being at different temperatures was investigated, with the wind contribution assumed to be null, which corresponds to the worst case scenario. We used the Fluent software to determine the thermodynamic parameters of the air within the ventilated layer and to investigate the impact of the various configurations mentioned above on the energy performance of the double skin roof using the CFD approach. It is a thorough modeling technique for solving the system of partial differential equations for mass, momentum, and energy conservation in an enclosed space, such as the solution domain shown in Figure 2. A finite volume technique was used to solve the time-averaged Navier-Stokes differential equations for steady and incompressible flows while considering turbulent phenomena. Turbulence modeling is especially important in CFD simulation since incorrect modeling can be a major source of inaccuracy. By Reynolds decomposition of the equations governing fluid motion, flow is analyzed in two parts, an average part, and a fluctuating component. Flow equations are then time averaged to yield an expression for the mean properties of the flow. All details concerning the state of the flow contained in instantaneous fluctuations are neglected. The process of time averaging introduces additional unknown terms in the conservation

equations. They are the so-called “Reynolds stresses”. The main task of turbulence modeling deals with the development of a computational procedure that enables the definition of these stresses. One of the most frequent types of turbulence models is the so-called "two-equation model." They also include two additional transport equations to represent the flow's turbulent properties. The standard k- "realizable" model was utilized in this paper, therefore the turbulent kinetic energy k and the turbulent dissipation rate are the additional transported variables. The precision of the flow inside the cavity is closely tied to the choice of this model (Shih *et al.*, 1995; Teodosiu, 2001). The impacts of the side walls were considered to be neglected because the ventilation channel length is significantly higher than its breadth, and the calculations were carried out assuming that the flow in the hollow is two-dimensional.

Within the solid parts, the no-slip condition is assumed and we performed a simulation by imposing an energy source reproducing the quantity of solar radiation absorbed by the outer surface of the roof.

In free convection, a constant relative pressure of 0 Pa has been imposed across all the surfaces surrounding outside the environment. These boundaries are assumed to be in ambient temperature but the exchange in long-wave radiation with the roof at the sky temperature. In the case of forced convection, we defined the inlet velocity and turbulence profile of the wind based on the measurements from our local weather station and considering the logarithmic law derived from the standard NF EN 1991-1-4 dated November 2005.

To resolve the near-wall flow, CFD simulations were run using the enhanced wall treatment approach, which aims to achieve near-wall modeling accuracy comparable to a two-layer approach (James and Webb 2004) without imposing a sufficiently fine mesh everywhere, which would have required too many computational resources. As a result, only the mesh in the near-wall region must be fine enough to allow full resolution of the viscosity-affected region.

A coarser mesh is allowed elsewhere. The demarcation of the two regions is determined by a non- dimensional wall distance y+ which is taken equal to 5 in this simulation. Meeting this requirement has been obtained as a result of a repeated mesh refinement

process performed on the cells sited along the channel boundaries. Such adaptation is iterated for each of the cases that have been simulated. An example of the results on mesh dimensions for such an iterative process is displayed in Fig. 3. The simulations were carried out by considering the air as a Newtonian fluid, incompressible, of constant viscosity and subjected to the gravity field. The discretization was based on the finite volume method and the resolution of the equations was based on the PISO algorithm in transient.

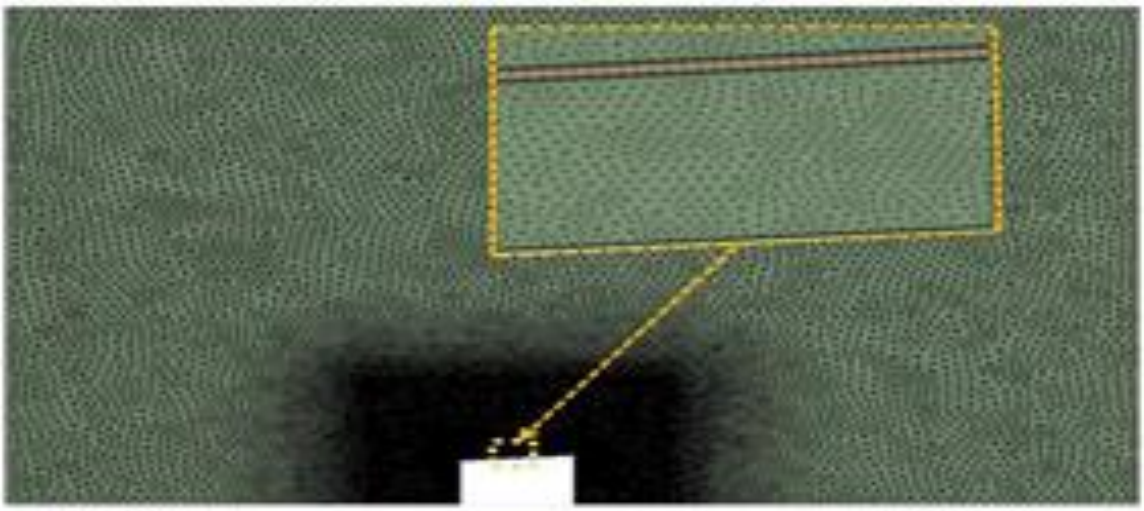

Figure 3: result of the meshing

The different tested cases are presented in Table 2. Three thicknesses of the air gap were tested for different solar radiation, and three insulation thicknesses were also studied. The outside temperature (Ta) is assumed to be equal to 40 °C and the internal temperature (Ti) is maintained at 26 °C. To study the effect of the emissivity (ε) of the internal surface of the roof screen, an extreme value of the emissivity (0.1) was applied to the case 4 to test the effect of a coating on the heat transfer through the roof.

Table 2. Studied Configurations

N°	d,	Insulation	di,	G,	ε	wind,
	m		M	W/m²		m/s
1	0.2	No	-	800	0.8	-
2	0.2	No	-	600	0.8	-
3	0.2	No	-	300	0.8	-
4	0.2	No	-	800	0.1	-
5	0.1	No	-	800	0.8	-
6	0.1	No	-	600	0.8	-
7	0.1	No	-	300	0.8	-
8	0.05	No	-	800	0.8	-
9	0.05	No	-	600	0.8	-
10	0.05	No	-	300	0.8	-
11	0.2	Yes	0.02	800	0.8	-
12	0.2	Yes	0.05	800	0.8	-
13	0.2	Yes	0.1	800	0.8	-
14	0.2	No	-	800	0.8	Yes

Where di is thickness of insulation (m), G is for incident global radiation (W/m²) and ε is for long-wave emissivity

3. Results and Discussions

3.1. Thermo-aeraulic performance of the roof

In the interests of simplification and simplicity, the flow in the air gap is analyzed based on velocities and temperature profile of air using the cases 1, 4, 5, 8, 13 and 14. The simulations show that the air goes through the cavity of the roof. Its temperature is close to the outdoor temperature. The objective is to obtain a roof with a low temperature. Figure 4 (b) reveals mainly, for all simulation that the outdoor air is heated along the roof cavity. As this air is heated, it rises by buoyancy forces before being evacuated by the exit of the cavity. This evacuation of air brings fresh air that is introduced into the cavity of the roof. The velocity contours in Fig. 4 (a) indicate, for all simulations, a higher air velocity near the roof cavity outlet. For the worst case, without wind effect, this speed remains low (maximum of 0.45 m/s). In addition, it is interesting to note some differences between the configurations. The temperature contours of case 4 are blue on the inner surface of the roof compared to the case.

Therefore, applying a treatment of low-emissivity in the internal surface of the screen in addition to the double skin roof can contribute to the reduction of the inner surface temperature. The heat transfer is thus essentially made by the radiation in the air gap. The choice of the surface to be treated is motivated by the fact that the ambient air is charged with the dust in Djibouti, so it is practically impossible to have such a low

emissivity on the other surfaces of the roof. Simulation 13 also shows that the use of insulation with respect to case 1 greatly reduces the temperature on the inner surface. Furthermore, the lower the thickness of the cavity, the more difficult it is for the air to evacuate the heat from the roof surfaces. From these results, it can be concluded that the double skin roof transfers its heat to the ambient air. This indicates a favorable behavior for the thermal discharge of the building's roof and thus being able to improve the thermal comfort inside and reduce the energy consumption due to the air conditioning.

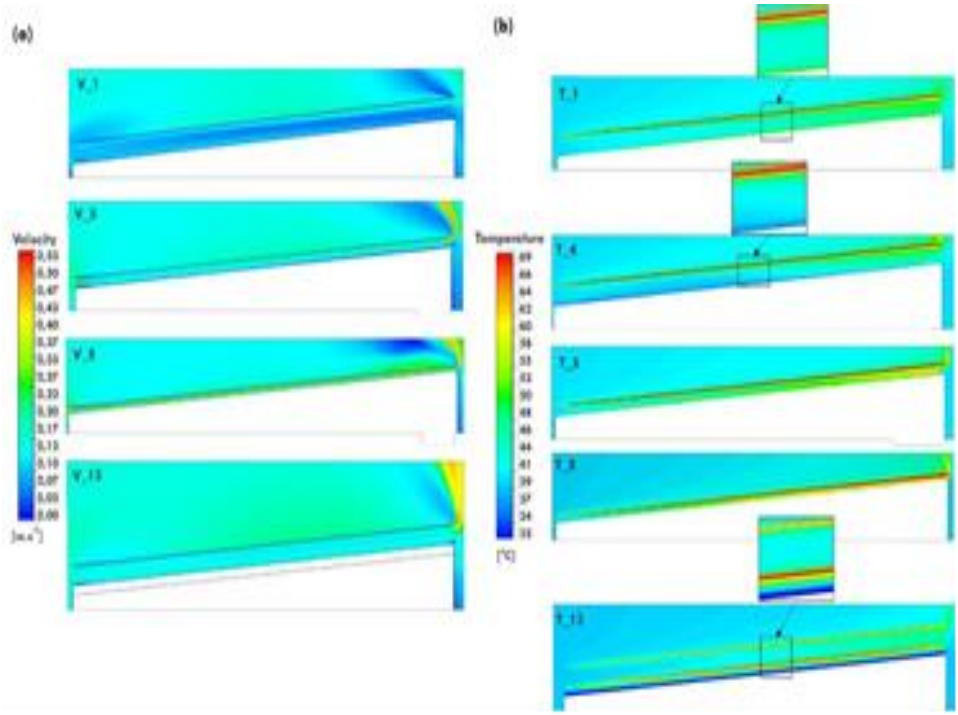

Figure 4. Thermo-aeraulic performance of the roof (a) higher air velocity near the roof cavity outlet (b) heated along the roof cavity

The temperature and air velocity profiles within the cavity are presented in Figure 5: Two, thermal and dynamic, boundary layers are developed in correspondence with the surfaces. We note that the air in the middle of the cavity remains at the outdoor temperature for the simple reason that the thermal boundary layer of the two surfaces have not merged and the temperature strongly increases near the upper surface of the roof for cases 1, 4, 5 and 13 (see Figure 5- (b), (d) and (f)). For case 8 where the cavity is thinner, the thermal boundary layers of the two surfaces are merged, and therefore, the air of the cavity is warmer. The average temperature of the upper surface of the roof varies from 367 K for case 4 to 357 K for case 1 while the temperature ranges from 308 K to 329 K for case 8.

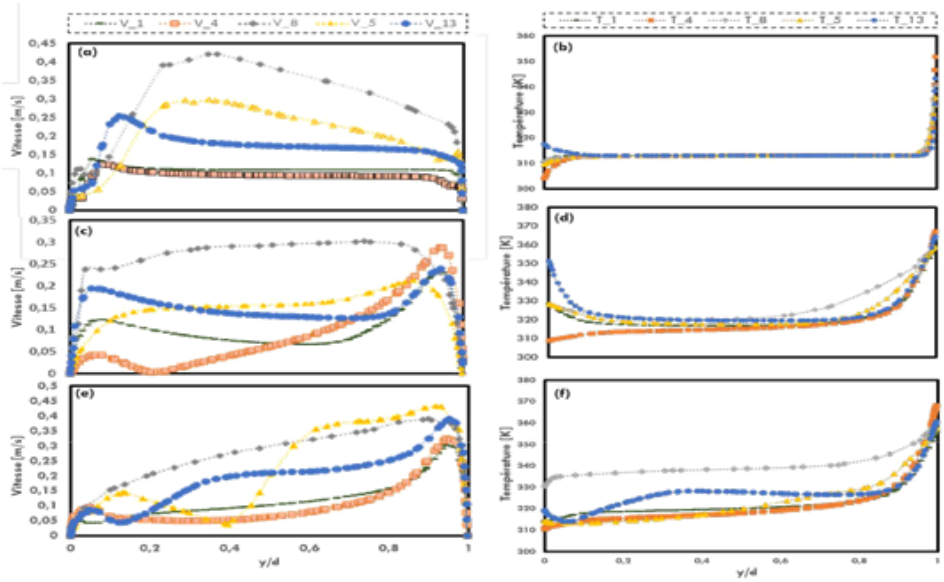

Figure 5: Velocity and temperature comparison for the case 1, 4, 5, 8, 13 (a) Velocity profiles at the inlet of the cavity (x/L=0); (b) Temperature profiles at the inlet of the cavity (x/L=0); (c) Velocity profiles at the middle of the cavity (x/L=0.5); (d) Temperature profiles at the middle of the cavity (x/L=0.5); (e) Velocity profiles at the outlet of the cavity (x/L=1); (f) Temperature profiles at the outlet of the cavity (x/L=1).

Although case 4 favours the reduction of the temperature of the inner surface of the roof, simulation 13 showed a better efficiency with a temperature of the inner surface of 300 K. The air velocity profile on each cross-section also shows two dynamic boundary layers which are developed along the inner and upper surfaces except for case 8 (Figure 5 (a), (c), (e)), with Zero value on both sides due to the no-slip boundary condition. The inlet velocities are disturbed by the edge effects and the air is accelerated in the outlet. Within the cavity, the maximum velocity is observed near the screen. This is caused by the buoyancy force, which is proportional to the difference between the plate's temperature and the outdoor temperature. The air increases along the direction of the motion with a maximum velocity of 0.25 m / s near the outlet and 0.45 m / s near the upper surface. Similar profiles were obtained for each simulation. We also carried out a simulation with the effect of the wind (case 14) to estimate its effects on the flow of air in the cavity (see Figure 6). This case is the most favourable configuration comparing to other cases. The velocity in Fig. 6 (a) and 6 (c) show velocities of up to 1.8 m / s in the cavity. The effects of the buoyancy force disappear with the contribution of the even if it weakly felt. It is also interesting to see an overpressure on the facade facing the wind (see Fig. 6 (b)).

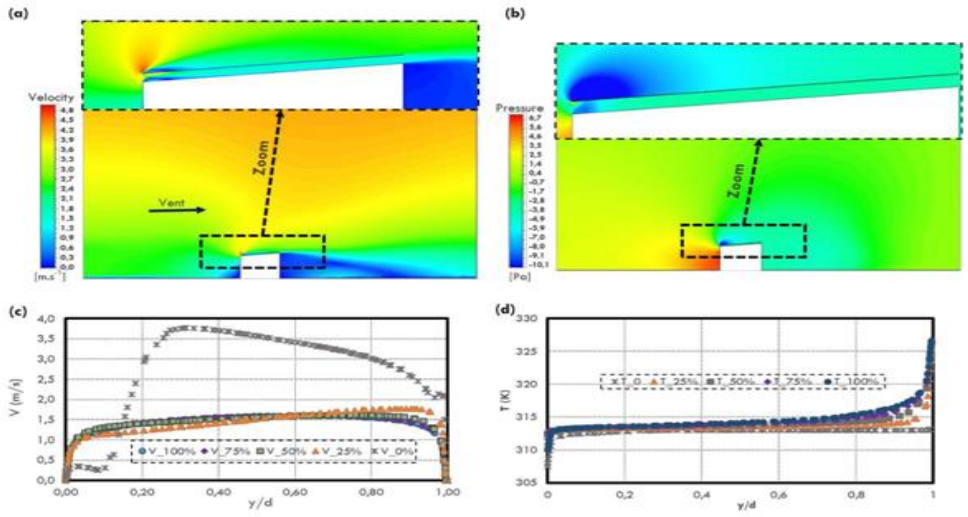

Figure 6: (a) Velocity contours for the case 14, (b) Pressure contours for the case 14, (c) Velocity profiles for the case 14, (d) Temperature profiles for the case 14;

V_0% → x/L=0; V_25%→ x/L=0.25; V_50%→ x/L=0.5; V_75% →x/L=0.75; V_100%→ x/L=1.

On the contrary, the leeward facade and the roof are in a depression. Consequently, there is a difference in pressure between the windward and leeward facades, allowing ventilation in the cavity. The temperature of the air in the middle of the channel remains at the outside temperature. The temperature of the screen varies from 313 K to 327 K along the cavity; while for the inner surface the temperature increases from 307 K to 313 K along the channel (see Figure 6 (d)).

3.2. Heat flux through the roof structure

To quantify the thermal efficiency of the ventilated double skin roof, it is necessary to compare the total flux through the inner surface for the different configurations presented above (see Figure 7). Only cases with the highest solar radiation value (G= 800 W / m²) in free convection are analysed and compared to the case “0”. This corresponds to the standard configuration shown in Figure 1 (b). It's important to note that using a ventilated roof reduces the heat flux into the building by nearly half. These findings appear to be in line with those given before. When compared to a typical roof, the system's inner surface has a low emissivity, which reduces heat input by 82 %. Case 13 has the best thermal performance, reducing total flow by 91% as compared to the standard roof.

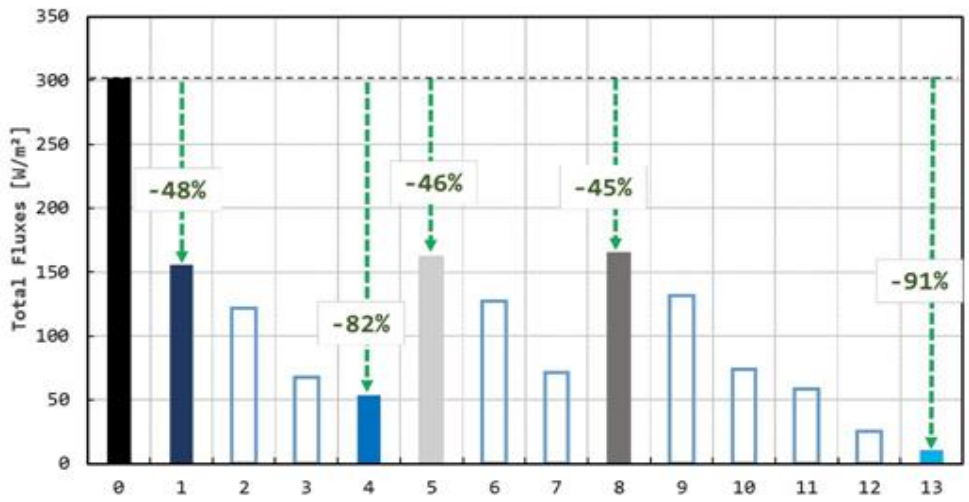

Figure 7: Heat flux comparison for different configuration

4. Conclusion

Numerous CFD simulations have been carried out to characterize the thermo-aeraulic behavior of a ventilated double-skinned roof under the climatic conditions of Djibouti. The results obtained by the CFD simulations evaluate the energy performance of the system by varying different parameters such as the thickness of the cavity, the insulation or the emissivity of the internal surface of the screen. The analysis concludes that in the worst case of free convection, the performance of the system is much better if, in addition to the double skin, the internal surface of the screen is treated. The thickness of the cavity seems to have a negligible impact on the total flux through the inner surface of the roof. The addition of the insulation considerably reduces the heat flux through the roof, and the best configuration, therefore, corresponds to case 13 with 91% reduction compared to the standard roof (good insulation and low emissivity). These results indicate the importance of using double-skin roofing as an effective way to minimize heat transfer through the roof, in hot areas such as Djibouti. Therefore, this bioclimatic technique might be considered an efficient and inexpensive technique to improve the energy performance of the building.

5. Conflict of interests

The authors state that they have no conflicting interests.

6. References

1. Abdou Idris O, I. AI, D. MS, K. AA (2016) Integration of Wind Flow into the Bioclimatic design in Djibouti. International Journal of Structural and Civil Engineering Research 5:87–92

2. ADME, (2013), Elaboration d'une stratégie et d'un plan d'action de maîtrise de l'énergie, Ministère de l'Energie en charge des Ressources Naturelles, Djibouti
3. Antvorskov S (2008) Introduction to integration of renewable energy in demand controlled hybrid ventilation systems for residential buildings. Building and Environment 43:1350–1353. doi: 10.1016/j.buildenv.2007.01.045
4. Biwole PH, Woloszyn M, Pompeo C (2008) Heat transfers in a double-skin roof ventilated by natural convection in summer time. Energy and Buildings 40:1487–1497. doi: 10.1016/j.enbuild.2008.02.004
5. Černe B, Medved S (2007) Determination of transient two-dimensional heat transfer in ventilated lightweight low sloped roof using Fourier series. Building and Environment42:2279–2288. doi: 10.1016/j.buildenv.2006.04.022.
6. CEN, EN 6946 - Building components and building elements – Thermal resistance and thermal transmittance - Calculation method. Brussels: European Committee for Standardization.
7. Chang P-C, Chiang C-M, Lai C-M (2008) Development and preliminary evaluation of double roof prototypes incorporating RBS (radiant barrier system). Energy and Buildings 40:140–147. doi: 10.1016/j.enbuild.2007.01.021
8. Ciampi M, Leccese F, Tuoni G (2005) Energy analysis of ventilated and microventilated roofs. Solar Energy 79:183–192. doi: 10.1016/j.solener.2004.08.014]
9. CSTB, (2002). Determination of the Thermal Performances of a Roof Ventilation System, E01-0005, Grenoble, France.
10. Dimoudi A, Androutsopoulos A, Lykoudis S (2006) Summer performance of a ventilated roof
11. component. Energy and Buildings 38:610–617. doi: 10.1016/j.enbuild.2005.09.006 DISED, (2015). Annuaire Statistique, Djibouti.
12. Fracastoro G. V., Gial L., Perino M. (1997), Reducing cooling loads with under roof air cavities, Proceedings of AIVC 18th Conference, "Ventilation and Cooling", Athens, Greece.
13. Gagliano A, Patania F, Nocera F, et al (2012) Thermal performance of ventilated roofs during summer period. Energy and Buildings 49:611–618. doi: 10.1016/j.enbuild.2012.03.007.
14. Hirunlabh J, Wachirapuwadon S, Pratinthong N, Khedari J (2001) New configurations of a roof solar collector maximizing natural ventilation. Building and Environment 36:383–391. doi: 10.1016/S0360-1323(00)00016-0
15. James DL, Webb SW (2004) Turbulent Natural Convection Heat Transfer in a Square Enclosure: Turbulence Model Comparisons. American Society of Mechanical Engineers, pp 193–199.
16. Khedari J, Yimsamerjit P, Hirunlabh J (2002) Experimental investigation of free convection in roof solar collector. Building and Environment 37:455–459. doi: 10.1016/S0360- 1323(01)00054-3
17. Lai C, Huang JY, Chiou JS (2008) Optimal spacing for double-skin roofs. Building and Environment 43:1749–1754. doi: 10.1016/j.buildenv.2007.11.008
18. Omar AI, Virgone J, Vergnault E, et al (2017) Energy Saving Potential with a Double-Skin Roof Ventilated by Natural Convection in Djibouti. Energy Procedia 140:361–373. doi: 10.1016/j.egypro.2017.11.149
19. Sandberg M, Moshfegh B (1998) Ventilated-solar roof air flow and heat transfer investigation. Renewable Energy 15:287–292. doi: 10.1016/S0960-1481(98)00175-X
20. Shih T-H, Liou WW, Shabbir A, et al (1995) A new k-ϵ eddy viscosity model for high reynolds number turbulent flows. Computers & Fluids 24:227–238. doi: 10.1016/0045-7930(94)00032-T
21. Teodosiu CI (2001) Modélisation des systèmes techniques dans le domaine des équipements des bâtiments à l'aide des codes de type CFD. Thesis, Lyon, INSA
22. Villi G, Pasut W, Carli MD (2009) CFD modelling and thermal performance analysis of a wooden ventilated roof structure. Build Simul 2:215–228. doi: 10.1007/s12273-009- 9414-7